Journal of Inorganic and General Chemistry
ZAAC
Zeitschrift für anorganische und allgemeine Chemie
DOI: 10.1002/zaac.202000414
ARTICLE

Chemical speciation in Gd–Cd–M (M = Zn, Au) quasicrystal approximants

Girma H. Gebresenbut,*[a] Cesar Pay Gómez,[a] Lars Eriksson,[b] and Ulrich Häussermann[b]

Dedicated to Professor Sven Lidin on the occasion of his 60th birthday.

We investigated the effect of partial replacement of Cd by M = Au and Zn in the crystal structure of the 1/1 Tsai-type quasicrystal approximant (AC) $GdCd_6$. Compositionally homogeneous single crystal samples $Gd(Cd_{0.87}Zn_{0.13(1)})_6$ and $Gd(Cd_{0.80}Au_{0.20(1)})_6$ were grown from melts $Gd_5(Cd_{0.8}Zn_{0.2})_{100}$ and $Gd_1(Cd_{0.9}Au_{0.1})_{100}$, respectively, and isolated by centrifugation. The M for Cd substitution in $GdCd_6$ is accompanied with a sizeable reduction of the cubic unit cell parameter, from 15.514(2) Å to 15.329(1) Å (Zn) and 15.314(1) Å (Au). Site preferences were established from single crystal X-ray diffraction data. A clear preference of atomic sites for Au and Zn is noted which is compared to earlier reported $Yb(Cd_{0.75}Mg_{0.25})_6$. Three and two out of in total seven crystallographic sites defining the Cd partial structure accept preferably metals more and less electronegative than Cd, respectively, and are classified as negatively and positively polarized sites in the binary 1/1 AC.

Introduction

The discovery of a series of binary Tsai-type quasicrystals (QCs) RE–Cd (RE = Gd–Tm)[1] fueled new interest in the magnetic properties of QCs and the fundamental question whether and how spins may order in a quasiperiodic atomic structure.[2] While long-range magnetic order has not yet been observed in Tsai-type QCs[3] antiferromagnetic (AFM) order has recently been reported for the compositionally and structurally related 1/1 ACs $RECd_{\sim 6}$.[4] Moreover, multiple anomalies in the temperature dependence of the magnetic susceptibility of $RECd_{\sim 6}$ with RE = Gd, Tb, and Ho indicate the existence of several distinct AFM phases.[4b] Against this background we deemed it interesting to investigate the consequences of partially substituting Cd by other metals in $GdCd_6$ in order to elucidate the effects on crystal chemistry and physical properties. In contrast with other RE–Cd ACs $GdCd_6$ displays a strict stoichiometry, 1:6, with no occupational disorder which somewhat simplifies the task.[5]

RE–Cd ACs (and also QCs) may be considered as polar intermetallic compounds, assuming formal oxidation of the RE metal and electron transfer to the more electronegative constituent, according to the Zintl concept. The site preference in multinary complex (polar) intermetallic compounds bears valuable information concerning their crystal chemistry, chemical bonding and physical properties. Site preferences in the crystal structure of inorganic materials has been introduced as "coloring problem" by Miller,[6] who also championed its application to polar intermetallics.[7]

Previous investigations focused on isovalent substitution by Mg. In particular, very recently Labib et al. reported on an extensive investigation of the phase relation between ACs and QCs in the ternary RE–Mg–Cd systems (RE = Y, Sm, Gd, Tb, Dy, Ho, Er, Tm), for which 20–25 % of Cd can be replaced by Mg,[8] and the magnetic properties of the ternary ACs and QCs.[9] Pay Gómez and Tsai studied the crystal chemical effects of Mg substitution in $YbCd_6$[10] and found a pronounced preference for Mg to locate on three of the seven sites constituting the Cd substructure. This picture was confirmed more recently by Yamada et al..[11] Moreover, these authors found slight compositional/occupational variations with respect to the previous model (with composition 1:6[5b]) and also, just recently, reported on intricate superstructure formation for $Yb(Cd_{0.9}Mg_{0.1})_{6.07}$ which is absent at higher Mg concentration.[12] Mg has a slighter larger size (atomic radius) than Cd (1.60 Å vs 1.51 Å),[13] but is considerably less electronegative (1.29 vs 1.52 on the Allen scale[14]). Here we report on the crystal chemical effect of Zn and Au substitution in $GdCd_6$. The corresponding compounds are the new ternary 1/1 AC phases $Gd(Cd_{0.87}Zn_{0.13(1)})$ and $Gd(Cd_{0.80}Au_{0.20(1)})_6$. Both Zn (1.37 Å) and Au (1.44 Å) have a smaller atomic size than Cd (1.51 Å). The electronegativity of Zn (1.59) is slightly higher, that of Au (1.92) is significantly higher. Together with the trends established for Mg substitution, it is hoped to obtain a more complete picture of the coloring problem in 1/1 ACs.

[a] Dr. G. H. Gebresenbut, Dr. C. Pay Gómez
Department of Chemistry-Ångström Laboratory
Uppsala University
751 21 Uppsala
Sweden
E-mail: girma.gebresenbut@kemi.uu.se
[b] Dr. L. Eriksson, Prof. U. Häussermann
Department of Materials and Environmental Chemistry
Stockholm University
S-10691 Stockholm
Sweden

Results and Discussion

Ternary $GdCd_6$ derivatives can be conveniently obtained as high quality and compositionally homogenous single crystal samples from solution growth experiments using Cd–M rich melts. We based our syntheses on the well-established Gd–Cd binary phase diagram.[1,15] Here we employed reaction mixtures $Gd_5(Cd_{0.8}Zn_{0.2})_{100}$ and $Gd_1(Cd_{0.9}Au_{0.1})_{100}$, which were heated to 800 °C and slowly cooled to 400 °C. Subsequently, crystals were isolated by centrifugation (see the experimental section for details). Figure 1 shows representatively crystal specimens and scanning electron microscope (SEM) images of polished grains used for energy despersive X-ray spectroscopy (EDX) analysis. From EDX, the M/Cd ratio is 0.16(1) and 0.28(1) for M = Zn and M = Au, respectively, which translates into the compositions $Gd(Cd_{0.86}Zn_{0.14(1)})_6$ and $Gd(Cd_{0.78}Au_{0.22(1)})_6$. One notices a significant deviation from the nominal M/Cd ratio of the reaction mixtures. Hence, one cannot assume that the solution growth of the AC phases proceeds according to a pseudo-binary phase diagram Gd–(Cd,M). Further syntheses attempts to increase Zn and Au concentrations in the ACs by increasing the M/Cd ratio of the starting nominal compositions were unsuccessful.

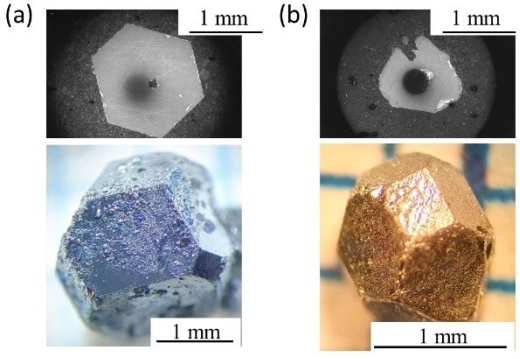

Figure 1. Scanning electron microscope SEM (top) and Optical photographs (bottom) of isolated grains of (a) $Gd(Cd_{0.80}Au_{0.20(1)})_6$ and (b) $Gd(Cd_{0.87}Zn_{0.13(1)})_6$ ACs. The SEM shows in-lens images taken from the specific grains shown at the bottom in the photographs after polishing. Typical facets of melt-grown 1/1 ACs, i.e. rectangular and irregular-hexagonal faces, are clearly visible in the photographs.

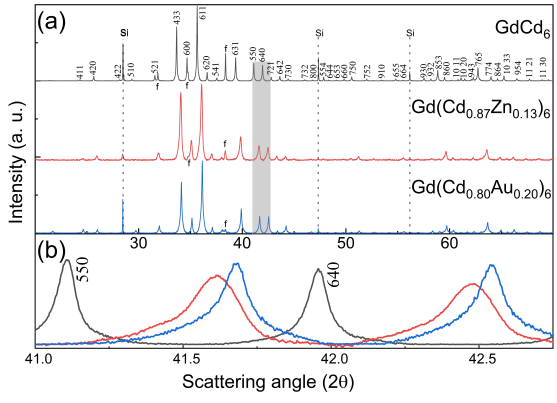

Figure 2. (a) PXRD patterns of $GdCd_6$ and the ternary ACs. (b) Zoomed in section of the marked (shadow-area) in (a) showing the systematic shift in diffraction peaks when Cd is partially replaced of Au and Zn. Diffraction background and peaks from Cu–$K_{\alpha 2}$ radiation have been subtracted from each pattern; Bragg peaks from internal Si-standard (Si) and residual melt (*f*) are indicated. Miller indices (hkl) are shown in (a).

Figure 2 compares the powder X-ray diffraction (PXRD) patterns of $GdCd_6$ with those of Zn and Au. One notices a sizable reduction of the cubic unit cell parameter (*a*), from 15.514(2) Å to 15.329(1) Å (Zn) and 15.314(1) Å (Au) as expected from the differences in atomic radii.

Crystals with suitable size for single crystal X-ray diffraction (SCXRD) measurements were selected from crushed mm-sized grains with well-developed facets. Data were refined against the well-established 1/1 AC model,[5b] see Table 1. In the 1/1 AC structure (space group $Im\bar{3}$) RE atoms are coordinated by 16 Cd atoms in the shape of a monocapped, double pentagonal antiprism. Alternatively, and more conveniently, the structure can be described as a packing of (Tsai) clusters consisting of concentric shells, cf. Figure 3.[16] The first shell corresponds to a pentagon dodecahedron which is defined by the positions Cd3

Table 1. Crystallographic data obtained from SCXRD refinements and EDX results. Lattice parameters obtained from PXRD experiment are included.

Parameters	Gd–Cd–Zn	Gd–Cd–Au
Ref. comp.	$Gd_1Cd_{5.24}Zn_{0.76(1)}$	$Gd_1Cd_{4.82}Au_{1.18(1)}$
Ref. comp. (formula)[a]	$Gd_1(Cd_{0.87}Zn_{0.13(1)})_6$	$Gd_1(Cd_{0.80}Au_{0.20(1)})_6$
EDX comp. (formula)[a]	$Gd_{1.0(1)}(Cd_{0.86}Zn_{0.14(1)})_6$	$Gd_{1.0(1)}(Cd_{0.78}Au_{0.22(1)})_6$
Molar mass (g/mol)	795.8	931.2
Temp. of meas. (°C)	20	20
Space group	$Im\bar{3}$ (204)	$Im\bar{3}$ (204)
a axis (Å) (SCXRD)	15.3156(2)	15.3663(2)
a axis (Å) (PXRD)	15.329(1)	15.314(1)
Cell volume (Å^3)	3592.54(8)	3628.34(8)
Z	24	24
Calc. density (g/cm^3)	8.82747	10.2275
Crystal colour	Metallic grey	Metallic grey
Abs. coeff. (mm^{-1})	31.999	55.721
Indep. Reflections	1730	1722
Obs. reflections[b]	25791	17272
R_{int} (obs/all)	3.75/3.93	5.73/5.74
Refined parameters	90	90
Redundancy	14.908	10
R1(obs/all)	2.54/4.05	3.43/3.74
*w*R2(obs/all)	5.22/5.44	9.44/9.49
GOF on F^2(obs/all)	2.01/1.88	2.98/2.89
$\Delta\rho_{max}$, $\Delta\rho_{min}$ (e/A^3)	2.53/-3.16	10.54[c]/–3.38

[a] measured compositions have been adapted to the chemical formula $A_1(B/C)_6$. [b] [$I > 3\sigma$ (I)]. [c] The large residual density is located at too short interatomic distance from the neighbouring atom (~1.2 Å from Cd4) and an attempt to include an atom resulted to unstable refinement; it could be then an artefact coming from intensities of a twinned crystal that was observed during data collection and large X-ray absorptions by Au and Cd.

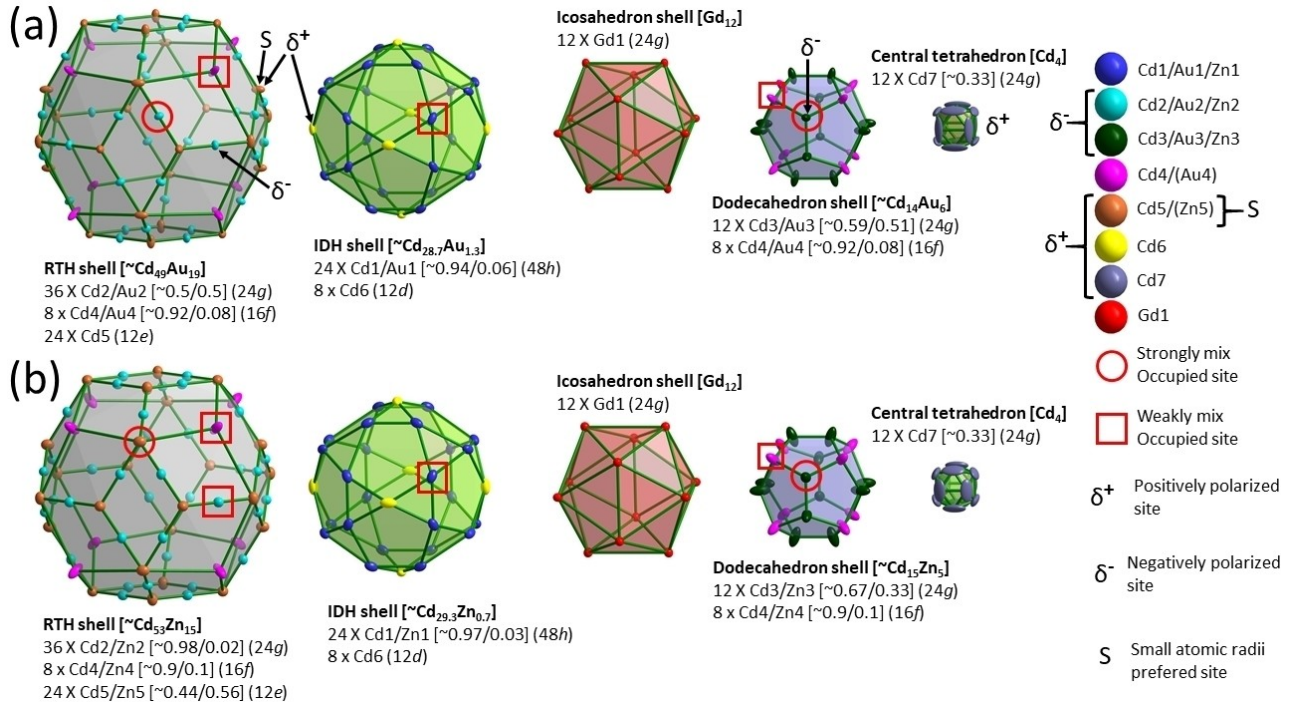

Figure 3. Plots of atomic structures obtained from SCXRD refinement results for (a) $Gd(Cd_{0.80}Au_{0.20(1)})_6$ and (b) $Gd(Cd_{0.87}Zn_{0.13(1)})_6$ ACs. All atomic positions except Cd7 have been displayed by thermal ellipsoids at the 95% probability level, for Cd7 50% was used. The polyhedra have been proportionally scaled with respect to each other. The content of each shell is described; atomic sites with strong and weak chemical disorder have been highlighted with circles and squares, respectively. Atomic sites with positive and negative polarizations and that prefers small size atoms are indicated in (a).

(24 *g*) and Cd4 (16 *f*). The next shell is an icosahedron built from the RE(Gd) atoms (position Gd1 (24 *g*)). The third shell is a 30 vertex icosidodecahedron (IDH), built from Cd1 and Cd6 atoms (positions 48 *h* and 12*d*, respectively). The outermost shell corresponds to a 32-vertex rhombic triacontahedron (RTH) defined by the positions Cd4 (16 *f*) and Cd5(24 *g*). Note that the Cd4 position is common to the dodecahedron and RTH shell. In addition, Cd2 atoms (*24 g*) are positioned on the edges between two Cd5 atoms. In the bcc 1/1 AC structure Tsai clusters are centered at the 2*a* position. Clusters are connected in the [100] direction by sharing common rhomboid faces defined by the Cd5 position and by interpenetrating along the [111] direction. The interpenetrating space (defined by Cd4 and Cd5 atoms, i.e. all RTH corners) has the shape of an obtuse rhombohedron.[17] Finally, Tsai clusters in $GdCd_6$ are centered by a Cd_4 tetrahedron (position Cd7), which at room temperature is orientationally disordered.[5b,18] Crystallographically, this Cd_4-tetrahedron is described by a site 24 *g*, with constrained occupancy 1/3, which emulates the disorder as three superimposed orientations.[5b]

The structure refinement results are summarized in Table 1 and atomic position parameters are listed in Table 2. The refined composition of the crystal matches closely to the EDX result. With respect to the average composition of the crystals, two positions have a clear preference to accept M. One (Cd3, dodecahedral shell) is common for both. Its site occupancy is about 50% Au and 33% Zn which, with respect to the average composition, corresponds to a very similar degree of speciation (enrichment by a factor 2–2.5). For $Gd(Cd_{0.87}Zn_{0.13(1)})_6$ the Cd5 position is preferred occupied by Zn (56%), whereas for $Gd(Cd_{0.80}Au_{0.20(1)})_6$ the Cd2 position is preferred occupied by Au (50%). Both positions belong to the RTH shell. The IDH shell remains essentially composed of Cd. Interestingly, the same is the case for the tetrahedral moiety at the cluster center. When comparing with $Yb(Cd_{0.75}Mg_{0.25})_6$[19] there are major differences. Mg substitution takes preferentially place at the Cd_4 tetrahedron (72% Mg) and also in the RTH shell (position Cd5 (87% Mg)) and the IDH shell (position Cd6 (70% Mg)).

Although site preference is a complex matter and could depend on more factors which are not discussed in the present study, our observations provide the following possible scenario of coloring for the 1/1 AC structure (cf. Figure 3): (1) Metals less electronegative than Cd (Mg) segregate into Cd_4 unit, the position on the two-fold rotational axes of the IDH shell, and one of the vertex positions of the RTH shell. Accordingly, these positions (Cd7, Cd6, and Cd5, respectively) are considered positively polarized in the Cd network of the $GdCd_6$ structure. (2) Metals more electronegative than Cd (Au) segregate into the dodecahedral shell and the mid-edge position of the RTH shell. Accordingly, these positions (Cd3 and Cd2, respectively) are considered negatively polarized in the Cd network of the $GdCd_6$ structure. (3) Both Zn and Mg both share preference for the Cd5 position, but are rather different in their electronegativity. At the same time, Zn has the smallest size of all considered

Table 2. Atomic parameters obtained from SCXRD refinements for $Gd(Cd_{0.80}Au_{0.20(1)})_6$ and $Gd(Cd_{0.87}Zn_{0.13(1)})_6$ ACs. Wyckoff positions (Wyck.), site occupancy factor (S.O.F.), atomic coordinates (x/a, y/a, z/a) and isotropic temperature parameters (U_{iso}) are indicated. All atomic positions are standardized.

	Gd–Cd–Au						Gd–Cd–Zn					
Wyck.	atom	S.O.F.	x/a	y/a	z/a	U_{iso}	atom	S.O.F.	x/a	y/a	z/a	U_{iso}
24 g	Gd1	1	0	0.18547	0.29856(6)	0.01213(17)	Gd1	1	0	0.18856	0.29933(4)	0.01473(12)
48 h	Cd1/Au1	0.9414/0.0586(38)	0.11529(6)	0.34234(6)	0.19995(6)	0.01808(20)	Cd1/Zn1	0.9695/0.0305(42)	0.11503(4)	0.34114(4)	0.19998(4)	0.02171(15)
24 g	Cd2/Au2	0.5007/0.4993(27)	0	0.40447	0.34316(6)	0.01436(19)	Cd2/Zn2	0.9798/0.0202(28)	0	0.40367	0.34895(5)	0.01735(19)
24 g	Cd3/Au3	0.4949/0.5051(30)	0	0.24309	0.09194(8)	0.0251(3)	Cd3/Zn3	0.6674/0.3326(29)	0	0.23719	0.09042(7)	0.03733(3)
16 f	Cd4/Au4	0.9172/0.0828(21)	0.16202	0.16202	0.16202(8)	0.0252(2)	Cd4/Zn4	0.8971/0.1029(21)	0.16127	0.16127	0.16127(5)	0.03277(16)
12 e	Cd5	1	0.18628	0.00000(12)	0.5	0.01823(4)	Cd5/Zn5	0.4362/0.5638(18)	0.19458	0.00000(9)	0.50000	0.02260(3)
12 d	Cd6	1	0.40783	0.00000(12)	0	0.01837(4)	Cd6	1	0.40451(7)	0.00000	0.00000	0.02650(3)
24 g	Cd7	0.3333	0.0000(7)	0.0714(8)	0.0883	0.163(7)	Cd7	0.3333	0.0000(4)	0.0901(5)	0.0637	0.1412(30)

substituting M. This may imply that for the RTH Cd5 position in addition to preference for less electronegative metals there may also be a simultaneous preference for accommodating smaller sized atoms. Similarly, one could argue that the dodecahedron Cd3 position (accepting preferably more electronegative metals) at the same time is also preferred for smaller sized M. Deeper insight with respect to atomic charges and volumes in the RE–Cd 1/1 AC crystal structure may be obtained from a Bader analysis[20] of DFT calculated charge densities (and using non-magnetic YCd_6 as a model system) and is subject to future investigations.

The title ternary compounds are considered terminal solid solutions of the $GdCd_6$ compound. Reactions using higher Au and Zn nominal starting concentrations, i.e. $(Gd_5(Cd_{0.5}Zn_{0.5})_{95})$ and $(Gd_5(Cd_{0.5}Au_{0.5})_{95})$, resulted in a mixture of AC phase and $Gd_2Zn_{15}Cd_2$ and $Gd_4Au_{10}Cd_3$ ternary phases, respectively. The lattice parameter of the AC phases obtained from the $Gd_5(Cd_{0.5}Zn_{0.5})_{95})$ and $(Gd_5(Cd_{0.5}Au_{0.5})_{95}$ reactions were not significantly different compared to those obtained from the initial reactions containing less M, indicating that the M/Cd ratio is essentially the same in both cases.

Conclusions

The ternary Tsai-type 1/1 ACs $Gd(Cd_{0.87}Zn_{0.13(1)})_6$ and $Gd(Cd_{0.80}Au_{0.20(1)})_6$ were grown from Cd-rich melts in order to investigate the effect of chemical substitution on the crystal chemistry. Faceted and mm-size ACs crystals were isolated from each compound and studied using SCXRD, PXRD and SEM/EDX techniques. Their compositions determined from EDX and the refinement of site occupancies were in good agreement. The site occupancies differ significantly from the average M/Cd composition of the crystals, indicating a strong coloring tendency of the Cd framework different sites. Interestingly, the central tetrahedron and the IDH shell remain essentially pure Cd positions, whereas in earlier investigated $Yb(Cd_{0.75}Mg_{0.25})_6$ there is a clear preference for Mg, which is less electronegative than Cd, to segregated there. In contrast, metals more electronegative than Cd have a clear preference to segregate into the dodecahedron and RTH shells.

Experimental Section

Starting chemicals were elemental granules commercially obtained from Chempur: Gd and Au with purity 99.99 at.%; Alfa Aldrich: Cd and Zn with purity 99.999 at.%. Alumina (Al_2O_3) crucibles, in the form of 'Canfield Crucible Sets (CCS)' were obtained from LSP Industrial Ceramics (USA). The CCS consists of two flat bottom cylindrical crucibles and an alumina frit-disc with holes of ~0.7 mm to 1 mm in diameter designed to separate the grains from the melt.[21] Two reactions, one for each compound $Gd(Cd_{0.87}Zn_{0.13(1)})_6$ and $Gd(Cd_{0.80}Au_{0.20(1)})_6$ were carried out using nominal compositions $Gd_5(Cd_{0.8}Zn_{0.2})_{100}$ and $Gd_1(Cd_{0.9}Au_{0.1})_{100}$, respectively. A total mass of 2 g were weighed for each reaction. The reactants were carefully weighed inside a glove box (Ar-atmosphere, <0.1 ppm O_2) loaded to CCSs which were then encapsulated inside stainless-steel ampules. A commercial multi-step programmable muffle furnace

was employed for setting the temperatures for the actual reactions. Typically, ampules were first heated to 800 °C during 5 h and kept for 10 h to ensure homogeneous melts. Then, the temperature was slowly lowered (1 °C/hr) to 400 °C to allow sufficient time for crystal growth and annealed at 400 °C for 50 h. Finally, reactions were terminated by isothermally centrifuging off excess melt at 400 °C.

The samples were studied with single crystal X-ray diffraction (SCXRD), powder X-ray diffraction (PXRD) and scanning electron microscopy (SEM) coupled with energy dispersive X-ray spectroscopy (EDX). A Bruker D8 single crystal X-ray diffractometer with Mo–K_α radiation ($K_\alpha = 0.71073$ Å) with an Incoatec Microfocus Source (IμS, beam size ≈100 μm at the sample position) and an APEX II CCD area detector (6 cm × 6 cm) was utilized to collect SCXRD intensities at room temperature. SCXRD data reduction and numerical absorption corrections were performed using the APEX III software from Bruker.[22] Both structure solution (by charge flipping) and refinements were performed using the software package JANA2006.[23] The charge flipping algorithm incorporated in the program Superflip was used to obtain structure solutions.[24] The crystal structures were visualized using Diamond 3.2 K4.[25] A Bruker D8 powder diffractometer with θ–2θ diffraction geometry and a Cu–Kα radiation ($K_{\alpha1} = 1.540598$ Å and $K_{\alpha2} = 1.544390$ Å) was used for collecting PXRD intensities at room temperature. PXRD data were analyzed with the HighScore Plus 3.0 software from PANalytical.[26] Powdered samples were applied to a zero-diffraction plate and diffraction patterns were measured in a 2θ range of 5–90°. In all PXRD experiments silicon powder was added as an internal standard. Scanning electron microscopy (SEM) investigations employed a Zeiss-Merlin instrument equipped with X-Max 80 mm^2 Silicon Drift EDX Detector with high sensitivity and at high count rates. Prior to the SEM/EDX experiments samples were cross section polished mechanically using Silicon carbide coated papers and significant portion of grains were removed from the surface. EDX data was collected with an acceleration voltage of 20 kV over larger areas (~1 × 1 mm) on at least 20 points for each sample.

Acknowledgements

We thank the Knut and Alice Wallenberg Foundation (grant number KAW 2018.0019).

Keywords: intermetallic phases · quasicrystal approximants · site preference · crystal chemistry · cluster

[1] A. Goldman, T. Kong, A. Kreyssig, A. Jesche, M. Ramazanoglu, K. Dennis, S. Bud'ko, P. Canfield, *Nat. Mater.* **2013**, *12*, 714–718.
[2] A. Goldman, *Sci. Technol. Adv. Mater.* **2014**, *15*, 044801.
[3] T. Kong, S. L. Bud'ko, A. Jesche, J. McArthur, A. Kreyssig, A. I. Goldman, P. C. Canfield, *Phys. Rev. B* **2014**, *90*, 014424.
[4] a) A. Kreyssig, G. Beutier, T. Hiroto, M. G. Kim, G. S. Tucker, M. d. Boissieu, R. Tamura, A. I. Goldman, *Philos. Mag. Lett.* **2013**, *93*, 512–520; b) A. Mori, H. Ota, S. Yoshiuchi, K. Iwakawa, Y. Taga, Y. Hirose, T. Takeuchi, E. Yamamoto, Y. Haga, F. Honda, R. Settai, Y. Ōnuki, *J. Phys. Soc. Jpn.* **2012**, *81*, 024720; c) R. Tamura, Y. Muro, T. Hiroto, K. Nishimoto, T. Takabatake, *Phys. Rev. B* **2010**, *82*, 220201.
[5] a) A. C. Larson, D. T. Cromer, *Acta Crystallogr. Sect. B* **1971**, *27*, 1875–1879; b) C. Pay Gómez, S. Lidin, *Phys. Rev. B* **2003**, *68*, 024203.
[6] G. J. Miller, *Eur. J. Inorg. Chem.* **1998**, *1998*, 523–536.
[7] a) Q. Lin, G. J. Miller, *Acc. Chem. Res.* **2018**, *51*, 49–58; b) M.-K. Han, E. Morosan, P. C. Canfield, G. J. Miller, *Z. Kristallogr. Cryst. Mater.* **2005**, *220*, 95.
[8] F. Labib, N. Fujita, S. Ohhashi, A.-P. Tsai, *J. Alloys Compd.* **2020**, *822*, 153541.
[9] F. Labib, D. Okuyama, N. Fujita, T. Yamada, S. Ohhashi, T. J. Sato, A.-P. Tsai, *J. Phys. Condens. Matter* **2020**, *32*, 415801.
[10] C. P. Gómez, A. P. Tsai, *C. R. Phys.* **2014**, *15*, 30–39.
[11] T. Yamada, H. Takakura, M. de Boissieu, A.-P. Tsai, *Acta Crystallogr. Sect. B* **2017**, *73*, 1125–1141.
[12] T. Yamada, *Philosophical Magazine* **2020**, 1–19.
[13] K. A. Gschneidner, J.-C. G. Bunzli, V. K. Pecharsky, *Handbook on the physics and chemistry of rare earths*, Elsevier, **2004**, p.
[14] L. C. Allen, *J. Am. Chem. Soc.* **1989**, *111*, 9003–9014.
[15] a) T. L. Reichmann, H. Ipser, *J. Alloys Compd.* **2014**, *617*, 292–301; b) G. Bruzzone, M. Fornasini, F. Merlo, *J. Less-Common Met.* **1971**, *25*, 295–301.
[16] C. P. Gómez, S. Lidin, *Angew. Chem. Int. Ed.* **2001**, *40*, 4037–4039; *Angew. Chem.* **2001**, *113*, 4161–4163.
[17] H. Takakura, C. Pay Gómez, A. Yamamoto, M. De Boissieu, A. P. Tsai, *Nat. Mater.* **2007**, *6*, 58–63.
[18] H. Euchner, T. Yamada, S. Rols, T. Ishimasa, Y. Kaneko, J. Ollivier, H. Schober, M. Mihalkovic, M. de Boissieu, *J. Phys. Condens. Matter* **2013**, *25*, 115405.
[19] F. Labib, D. Okuyama, N. Fujita, T. Yamada, S. Ohhashi, D. Morikawa, K. Tsuda, T. J. Sato, A.-P. Tsai, *J. Phys. Condens. Matter* **2020**, *32*, 485801.
[20] R. Bader, *Atoms in molecules: a quantum theory,* Clarendon Press, Oxford **1990**, p. 438.
[21] P. C. Canfield, *Rep. Prog. Phys.* **2019**, *83*, 016501.
[22] A. SAINT, Bruker Analytical X-ray Systems Inc., Madison, WI **2014**.
[23] V. Petříček, M. Dušek, L. Palatinus, *Z. Kristallogr. Cryst. Mater.* **2014**, *229*, 345–352.
[24] L. Palatinus, G. Chapuis, *J. Appl. Crystallogr.* **2007**, *40*, 786–790.
[25] H. Putz, K. Brandenburg, *Crystal Impact-GbR, Kreuzherrenstr* **2006**, *102*, 53227.
[26] T. Degen, M. Sadki, E. Bron, U. König, G. Nénert in *The HighScore suite, Vol.* Supplement S2 Volume 29, **2014**, pp. S13–S18.

Manuscript received: November 5, 2020
Revised manuscript received: December 22, 2020